Cell Host & Microbe
Article

The *Legionella* Effector RidL Inhibits Retrograde Trafficking to Promote Intracellular Replication

Ivo Finsel,[1,6] Curdin Ragaz,[1,5,6] Christine Hoffmann,[1] Christopher F. Harrison,[1] Stephen Weber,[1] Vanessa A. van Rahden,[2] Ludger Johannes,[3,4] and Hubert Hilbi[1,*]
[1]Max von Pettenkofer Institute, Ludwig-Maximilians University Munich, 80336 Munich, Germany
[2]Institute for Human Genetics, University Hospital Hamburg-Eppendorf, 20246 Hamburg, Germany
[3]CNRS UMR144, France
[4]Institut Curie, Centre de Recherche, Traffic, Signaling, and Delivery Laboratory, 75248 Paris Cedex 05, France
[5]Present address: F. Hoffmann-La Roche Ltd., PTDSC2H, 4070 Basel, Switzerland
[6]These authors contributed equally to this work
*Correspondence: hilbi@mvp.uni-muenchen.de
http://dx.doi.org/10.1016/j.chom.2013.06.001

SUMMARY

The bacteria causing Legionnaires' disease, *Legionella pneumophila*, replicate intracellularly within unique *Legionella*-containing vacuoles (LCVs). LCV formation involves a type IV secretion system (T4SS) that translocates effector proteins into host cells. We show that the T4SS effector RidL localizes to LCVs, supports intracellular bacterial growth, and alters retrograde trafficking, in which selected proteins are transported from endosomes to the Golgi. The retromer complex that mediates retrograde trafficking localizes to LCVs independently of RidL and restricts intracellular bacterial growth. RidL binds the Vps29 retromer subunit and the lipid PtdIns(3)*P*, which localizes retromer components to membranes. Additionally, specific retromer cargo receptors and sorting nexins that mediate protein capture and membrane remodeling preferentially localize to LCVs in the absence of *ridL*. Ectopic RidL production inhibits retrograde trafficking, and *L. pneumophila* blocks retrograde transport at endosome exit sites in a *ridL*-dependent manner. Collectively, these findings suggest that RidL inhibits retromer function to promote intracellular bacterial replication.

INTRODUCTION

Inhalation of the amoeba-resistant environmental bacterium *Legionella pneumophila* can cause a severe pneumonia termed Legionnaires' disease (Hilbi et al., 2011a; Newton et al., 2010). *L. pneumophila* is an accidental human pathogen that employs a conserved mechanism to replicate intracellularly within both environmental protozoa and alveolar macrophages. The bacteria form a distinct, membrane-bound compartment, the replication-permissive *Legionella*-containing vacuole (LCV) (Hilbi and Haas, 2012; Hubber and Roy, 2010; Isberg et al., 2009). LCVs intercept the early secretory pathway and finally merge with the endoplasmic reticulum (ER). Proteomic analysis of purified LCVs revealed the presence of small host GTPases implicated in the secretory (Arf1, Rab1, and Rab8) and endosomal (Rab7 and Rab14) vesicle trafficking pathways, indicating that the pathogen vacuole interacts with these trafficking routes (Urwyler et al., 2009).

LCVs are formed in a robust and complex process involving the Icm/Dot type IV secretion system (T4SS) and close to 300 different translocated effector proteins that are thought to subvert host signaling and vesicle transport (Hubber and Roy, 2010; Weber et al., 2009b). Some Icm/Dot substrates target host small GTPases, phosphoinositide (PI) lipids, or the ubiquitinylation machinery, yet the function of most of these putative effector proteins remains elusive.

The proteins Lpg2311 (Ceg28) and Lpg2511 (SidC) encoded by *L. pneumophila* strain Philadelphia 1 show similarity to interaptin (Chien et al., 2004), a 204 kDa *Dictyostelium discoideum* protein that localizes to intracellular membranes, including the ER (Rivero et al., 1998). The 106 kDa protein SidC (substrate of Icm/Dot transporter) (Luo and Isberg, 2004) is an effector that anchors via phosphatidylinositol 4-phosphate (PtdIns(4)*P*) to the LCV membrane and promotes the recruitment of ER to LCVs (Brombacher et al., 2009; Ragaz et al., 2008; Weber et al., 2006). The 131 kDa protein Lpg2311 is encoded by *ceg28* (coregulated with effector-encoding genes), regulated by the two-component response regulator PmrA (Zusman et al., 2007), and translocated by the Icm/Dot T4SS (Zhu et al., 2011; Huang et al., 2011).

The eukaryotic retrograde vesicle trafficking pathway promotes transport from early, late, and recycling endosomes to the *trans* Golgi network (TGN) and through the Golgi apparatus to the ER (Bonifacino and Hurley, 2008; Cullen and Korswagen, 2012; Lowe, 2005; Seaman, 2005). A well-characterized substrate of the retrograde transport route is the transmembrane cation-independent mannose 6-phosphate receptor (CIMPR). CIMPR binds mannose 6-phosphate on acidic hydrolases, delivers the cargo from the TGN to endosomal compartments, and, after ligand release into the lysosomal lumen, is recycled back via the retrograde route to the TGN. Retrograde sorting of CIMPR requires a protein complex termed the retromer (Arighi et al., 2004; Seaman, 2004).

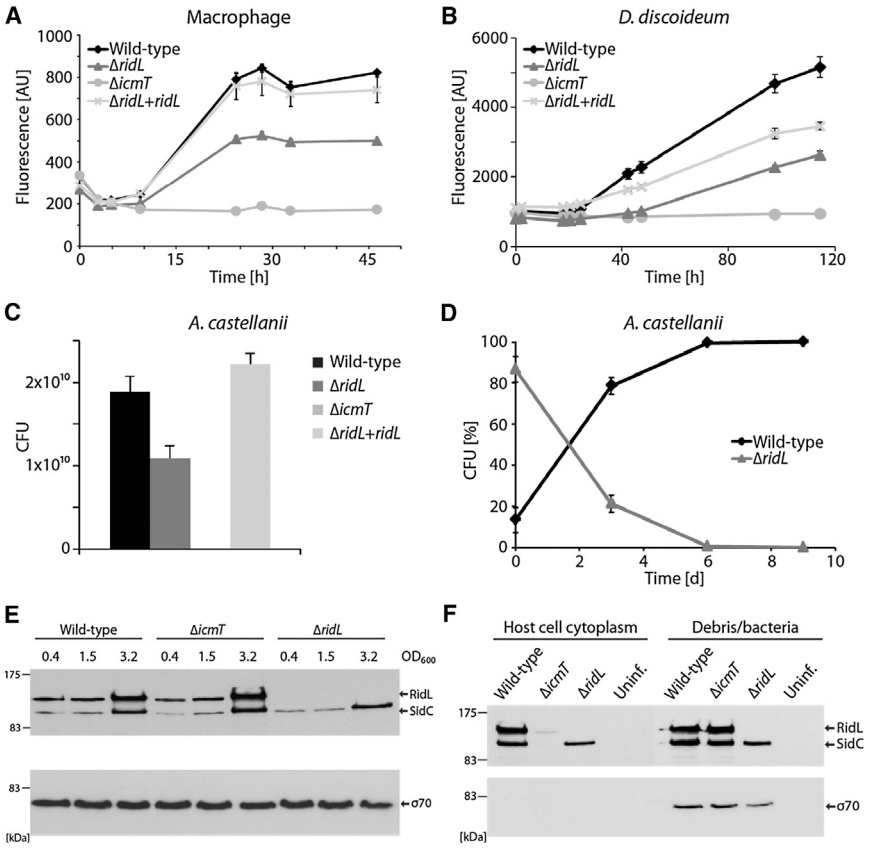

Figure 1. The *L. pneumophila* Icm/Dot Substrate RidL Promotes Host Cell Interactions

(A–C) RAW 264.7 macrophages (MOI 5) (A), *D. discoideum* (MOI 5) (B), or *A. castellanii* (MOI 20) (C) were infected with *L. pneumophila* WT, Δ*icmT*, Δ*ridL* harboring pNT28 (GFP), or Δ*ridL* harboring pIF009 (GFP and RidL). Intracellular growth (or killing of Δ*icmT*) was determined by fluorescence at the time points indicated (A and B) or by cfu 2 days postinfection (C). Graphs indicate means and SDs of triplicates (Student's t test, which was used throughout the study) or mean fluorescence and SDs of 12 samples per strain. AU, arbitrary units.

(D) Competition defect of Δ*ridL*. *A. castellanii* was coinfected (1:10; MOI 0.01 and MOI 0.1) with *L. pneumophila* WT and Δ*ridL* and grown at 37°C for 9 days. Every third day, supernatant and lysed amoeba were diluted 1:1000, fresh amoeba were infected (1:5), and aliquots were plated on charcoal yeast extract agar plates ± Km to determine cfu. Data are means and SDs of triplicates.

(E) Growth-phase-dependent production of RidL, SidC, or sigma factor σ70 (loading control) was quantified by western blot in *L. pneumophila* WT, Δ*icmT*, or Δ*ridL* grown to early (OD_{600} 0.4), midlog (OD_{600} 1.5), or stationary (OD_{600} 3.2) phase.

(F) Icm/Dot-dependent translocation of RidL. RAW 264.7 macrophages infected with *L. pneumophila* WT, Δ*icmT*, or Δ*ridL* (MOI 50, 1 hr) were solubilized with saponin and fractionated. Translocation and subcellular localization of RidL and SidC were determined by western blot.

Data in (A)–(F) are representative of three independent experiments. See also Figure S1.

The retromer consists of the heterotrimeric cargo recognition subcomplex Vps26-Vps29-Vps35 and a membrane-deforming subcomplex comprised of dimeric sorting nexins (SNXs). The retromer complex is essential for retrograde trafficking, along with other components, including the phosphatidylinositol 3-kinase (PI3K) Vps34 as well as the inositol-polyphosphate 5-phosphatases OCRL and INPP5B (Bonifacino and Hurley, 2008; Cullen and Korswagen, 2012; Lowe, 2005; Seaman, 2005). Whereas SNXs localize to membranes by binding to PtdIns(3)*P*, the cargo recognition subcomplex is recruited to membranes by activated Rab7 (Rojas et al., 2008; Seaman et al., 2009). The cargo recognition subcomplex binds the cytoplasmic part of transmembrane cargo receptors and subsequently interacts with SNXs, leading to compartment tubulation and vesicle fission (Bonifacino and Rojas, 2006; Cullen and Korswagen, 2012; Johannes and Popoff, 2008).

Different cargoes of the retrograde trafficking pathway require different transport factors. Bacterial toxins (shiga toxin and cholera toxin) and plant toxins (ricin), as well as some viruses (HIV and SV40), hijack the retrograde pathway to access the host cell cytoplasm or promote other steps of the infection process (Bonifacino and Rojas, 2006; Johannes and Popoff, 2008). Here, we show that the *L. pneumophila* Icm/Dot substrate RidL (Lpg2311/Ceg28) binds the retromer cargo recognition subcomplex, inhibits retrograde trafficking, and promotes intracellular bacterial replication.

RESULTS

The *L. pneumophila* Icm/Dot Substrate RidL Promotes Host Cell Interactions

To analyze the functions of *L. pneumophila* Lpg2311/Ceg28 genetically, we constructed the corresponding deletion mutant (strain CR06, Table S1 available online). On the basis of the properties of Lpg2311/Ceg28 described here, we propose to term the protein RidL (retromer interactor decorating LCVs). An *L. pneumophila* strain lacking *ridL* (Δ*ridL*) grew at wild-type (WT) rates in yeast extract broth (data not shown) and was taken up by macrophages or *D. discoideum* as efficiently as WT bacteria (Figure S1). However, *L. pneumophila* Δ*ridL* was impaired for intracellular growth in RAW 264.7 macrophages (Figure 1A), *D. discoideum* (Figure 1B), and the natural protozoan host *Acanthamoeba castellanii* (Figure 1C), as determined by GFP fluorescence or colony-forming units (cfu). The growth defect was at least partially complemented by providing the *ridL* gene on a plasmid. Moreover, upon coinfection of Δ*ridL* with WT *L. pneumophila*, the mutant strain was outcompeted within 6 days (Figure 1D). In summary, RidL promotes intracellular replication of *L. pneumophila* in protozoan and metazoan phagocytes.

The *ridL* gene was preferentially expressed in the late postexponential growth phase (Figure 1E), a feature of PmrA targets (Zusman et al., 2007) and other genes encoding Icm/Dot substrates such as SidC (Luo and Isberg, 2004). RidL was produced

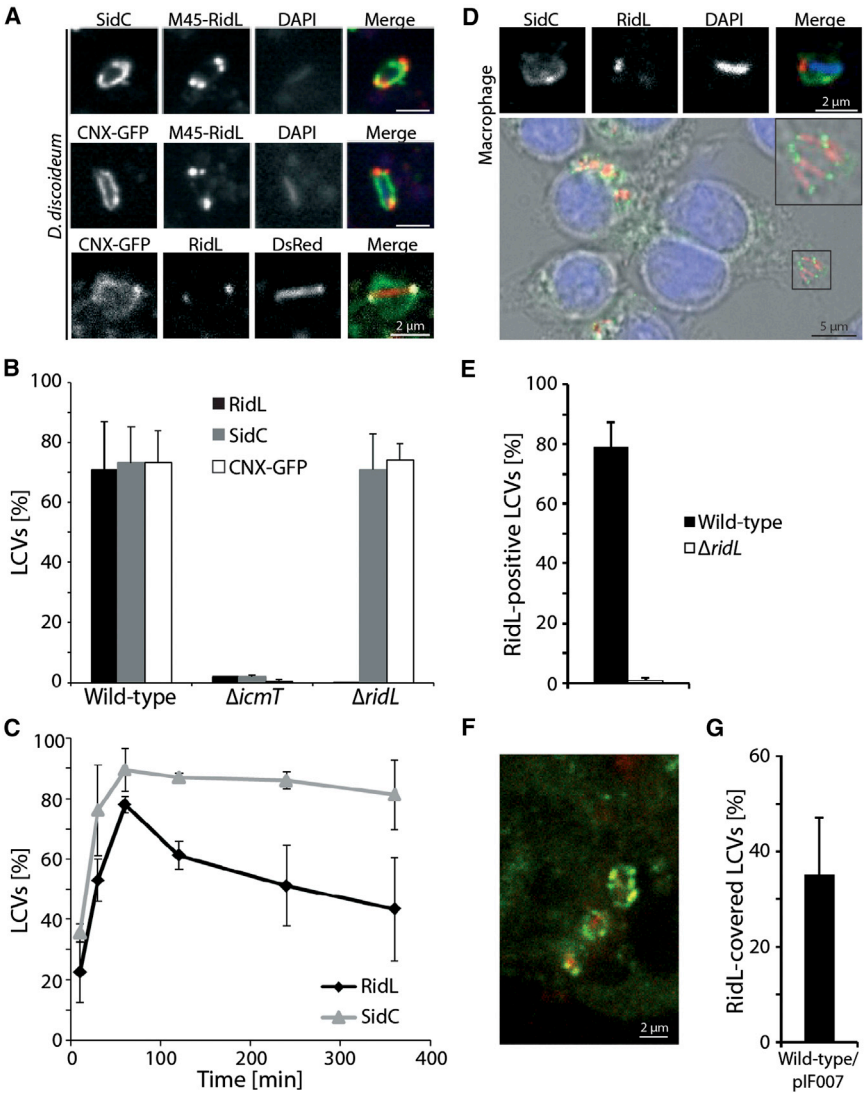

Figure 2. Localization of RidL on LCV Membranes in *D. discoideum* or Macrophages

(A and B) RidL localizes to LCVs in *D. discoideum*. WT or calnexin-GFP producing *D. discoideum* was infected (MOI 50, 1 hr) with *L. pneumophila* WT harboring pCR38 (M45-RidL) or pSW001 (DsRed). M45-tagged (A) or endogenous RidL and SidC (B) were localized by immunofluorescence using antibodies against M45, RidL, or SidC (where indicated, bacteria are stained with DAPI). Data represent means and SDs of three independent experiments. The scale bar represents 2 μm.

(C) RidL dynamics on LCVs. Calnexin-GFP producing *D. discoideum* was infected (MOI 10, 1 hr) with *L. pneumophila* WT/pSW001 (DsRed), and endogenous RidL or SidC on LCVs was determined by immunofluorescence. Data represent means and SDs of two independent experiments (50–100 LCVs each).

(D and E) RidL localizes to LCV in macrophages. RAW 264.7 macrophages were infected (MOI 10, 1 hr) with WT *L. pneumophila* harboring pCR34 (M45-SidC) or pSW001 (DsRed). Endogenous RidL on LCVs in homogenates (D, upper panels) or intact cells (D, lower panel, and E) was analyzed by immunofluorescence (where indicated, bacteria are stained with DAPI). Data represent means and SDs of three independent experiments (>50 LCVs each).

(F and G) Distribution of overproduced RidL on LCVs. RAW 264.7 macrophages were infected (MOI 10, 1 hr) with WT *L. pneumophila*/pIF007 (DsRed and RidL), and RidL on LCVs was visualized by immunofluorescence microscopy.

Data represent means and SDs of three independent experiments (>40 LCVs each). See also Figure S2.

by nine clinical and environmental *L. pneumophila* strains tested, but not by several other *Legionella* spp. (Figure S1), and the gene is present in the genome of *L. pneumophila*, *L. longbeachae* as well as *L. drancourtii*. Finally, the Icm/Dot-dependent translocation of RidL and SidC into the cytoplasm of RAW 264.7 macrophages was confirmed with adenylate cyclase fusion proteins (Figure S1) or saponin detergent extraction and subcellular fractionation (Figure 1F).

Localization of RidL on LCV Membranes in *D. discoideum* or Macrophages

The cellular localization of translocated RidL was analyzed in *D. discoideum* producing the ER and LCV membrane marker calnexin-GFP. Upon infection with *L. pneumophila*, M45-tagged or endogenous RidL localized to the LCV membrane in punctate aggregates juxtaposed with the bacterial poles (Figure 2A). At the same time, the LCV membrane was uniformly decorated by the PtdIns(4)*P*-binding effector SidC and calnexin. One hour after infection, approximately 70% of LCVs scored positive for RidL, SidC, and calnexin, and the accumulation of these proteins on LCVs was strictly dependent on the Icm/Dot T4SS (Figure 2B; see also Figure S2).

In the absence of *ridL*, a similar number of LCVs stained positive for SidC and calnexin, suggesting that RidL neither alters the pool of PtdIns(4)*P* on LCV membranes nor affects the interaction of LCVs with the ER (Figure 2B). The percentage of WT LCVs decorated with RidL or SidC reached a maximum of 80%–90% within 1 hr after infection, and approximately 45% LCVs still carried RidL after 6 hr, whereas the level of SidC-positive LCVs remained constant (Figure 2C). As in *D. discoideum*, approximately 80% of LCVs in macrophages were decorated with endogenous RidL localizing in punctate aggregates juxtaposed with the bacterial poles (Figures 2D and 2E).

To test whether the overproduction of RidL alters its distribution on LCVs, we used an *L. pneumophila* strain harboring the plasmid pIF007, which produces approximately 200× more RidL than WT bacteria (Figure S2). Under these conditions, more than 35% of the RidL-positive LCVs in macrophages were covered with RidL on extended areas of the membrane (Figure 2F, 2G). These findings suggest that RidL binds a receptor that localizes throughout the LCV membrane and is not only adjacent to the bacterial poles. Altogether, different approaches

indicate that RidL is an Icm/Dot-translocated *L. pneumophila* effector protein that localizes to LCV membranes in amoeba and macrophages already at an early phase during LCV formation.

RidL Binds to Subunit Vps29 of the Eukaryotic Retromer

To obtain insights into eukaryotic targets of RidL or SidC, we covalently coupled the purified proteins to beads and incubated the beads with lysate from RAW 264.7 macrophages or *D. discoideum* (Figure 3A). Dominant macrophage proteins specifically retained by RidL, but not by SidC, were identified by mass spectrometry as the Vps35 (92 kDa), Vps26 (38 kDa), and Vps29 (20 kDa) subunits of the heterotrimeric eukaryotic retromer cargo recognition subcomplex. Densitometric analysis of the protein bands indicated a stoichiometry of approximately 1:1:1 (data not shown), corresponding to the subunit ratio in the native retromer subcomplex. Upon incubation of RidL-conjugated beads with *D. discoideum* lysate, a dominant and specifically retained protein was identified as the Vps35 retromer component (Figure 3A), confirming the findings with macrophage lysate. Finally, the bait proteins RidL or SidC were also identified in the eluates from beads.

To assess the binding of RidL to individual subunits of the retromer complex, we purified GST fusion proteins of the Vps26 or Vps29 subunits to homogeneity, incubated the proteins with *L. pneumophila* lysate, and precipitated them with glutathione sepharose beads (Figure 3B). Western blot with an antibody against RidL revealed that RidL exclusively binds the Vps29 but not the Vps26 retromer subunit in vitro. Similar results were obtained with purified His-tagged RidL produced in *E. coli*, suggesting that RidL can bind Vps29 directly and in absence of other *L. pneumophila* factors (data not shown).

Inhibition of Retrograde Trafficking Promotes *L. pneumophila* Replication

Given that RidL binds the retromer Vps29 subunit, we tested whether the silencing of components of the retrograde vesicle trafficking pathway by RNAi affects the intracellular replication of *L. pneumophila* in HeLa cells. As a control, the small GTPase Arf1 was depleted, which reduced the cfu count of *L. pneumophila* approximately 2.5-fold (Figure 3C; see also Figure S3). Silencing of the retromer subunits Vps26A/Vps26B or Vps29, the retrograde cargo receptor CIMPR, the PI 5-phosphatases OCRL or INPP5B, or PI3K resulted in the recovery of about twice as many cfu WT *L. pneumophila* in comparison to the control with scrambled small interfering RNA (siRNA). Unexpectedly, RNAi targeting Vps35 did not affect intracellular growth of *L. pneumophila*. However, although this treatment depleted Vps35-encoding messenger RNA (mRNA), 20%–40% of the corresponding protein remained (Figure S3), suggesting that residual Vps35 masked RNAi.

Furthermore, treatment with a mixture of four different siRNA oligonucleotides targeting SNX1, −2, −3, or −5 alone or two of the SNXs in combination did not affect the intracellular growth of *L. pneumophila* (Figure S3). Finally, the silencing of retrograde trafficking components not only increased the cfu count for WT but also for Δ*ridL* mutant *L. pneumophila* (Figure S3).

The role of retrograde trafficking for intracellular replication of *L. pneumophila* was also determined with the use of fibroblasts from Lowe syndrome patients suffering from a loss-of-function mutation in the *OCRL* gene implicated in retrograde transport (Lowe, 2005). In these cells, the cfu count of WT bacteria was approximately doubled in comparison to fibroblasts from healthy donors (Figure S3). The cfu count of Δ*icmT* mutant bacteria decreased to a similar extent in fibroblasts from either source (Figure S3), suggesting that OCRL does not affect bacterial killing. In summary, the functional impairment of different components of the retrograde pathway augmented *L. pneumophila* cfu, suggesting that retrograde trafficking restricts intracellular bacterial growth.

The Retromer Cargo Recognition Subunits Localize to LCVs

To address whether retromer components localize to LCVs, we produced GFP fusion proteins of Vps26 or Vps29 in *D. discoideum* and analyzed the localization of Vps35 by immunofluorescence microscopy in RAW 264.7 macrophages. The retromer subunits localized to the LCV membrane in a strictly Icm/Dot-dependent manner (Figures 3D and 3E; see also Figure S3). In homogenates of infected *D. discoideum*, approximately 70% of LCVs containing WT *L. pneumophila* stained positive for Vps26, Vps29, or calnexin. In macrophages, about 30% of LCVs containing WT bacteria scored positive for Vps35, in comparison to approximately 60% of LCVs that were decorated with early endosomal antigen 1 (EEA1). In the absence of *ridL*, the accumulation of the retromer cargo recognition subunits on LCVs was not significantly affected in either *D. discoideum* or macrophages (Figures 3D and 3E; see also Figure S3), indicating that RidL is dispensable for the recruitment and assembly of the subcomplex. Thus, the heterotrimeric retromer cargo recognition subcomplex localizes to LCVs in an Icm/Dot-dependent, but RidL-independent, manner.

RidL Inhibits the Accumulation of Retrograde Cargo Receptors on LCVs

To determine whether RidL modulates the LCV host factor composition, we used fluorescence microscopy to assess different proteins localizing to LCVs harboring either WT or Δ*ridL* *L. pneumophila*. Vps10, a *D. discoideum* homolog of mammalian sortilin, or CIMPR are cargo receptors recycled via retrograde transport. The number of LCVs scoring positive for these cargo receptors significantly increased in absence of *ridL*; whereas 40%–45% of LCVs in *D. discoideum* or macrophages infected with *L. pneumophila* Δ*ridL* scored positive for Vps10 (Figure 3D) or CIMPR (Figure 3E), respectively, only 25%–30% of LCVs in phagocytes infected with WT bacteria scored positive for the cargo receptors. These results suggest that RidL modulates retrograde trafficking.

Other factors implicated in retrograde vesicle trafficking identified on LCVs include the PI 5-phosphatase Dd5P4/OCRL, corroborating the notion that the pathogen vacuole communicates with the retrograde pathway. However, this LCV marker, as well as others, such as the small secretory GTPases Rab1 and Rab8 or the endosomal markers Rab7, Rab14, and the putative copper transporter p80 (Clemens et al., 2000; Kagan et al., 2004; Urwyler et al., 2009; Weber et al., 2009a), did not accumulate to a different extent on LCVs harboring either WT or Δ*ridL* *L. pneumophila* (Figure S3). These results suggest

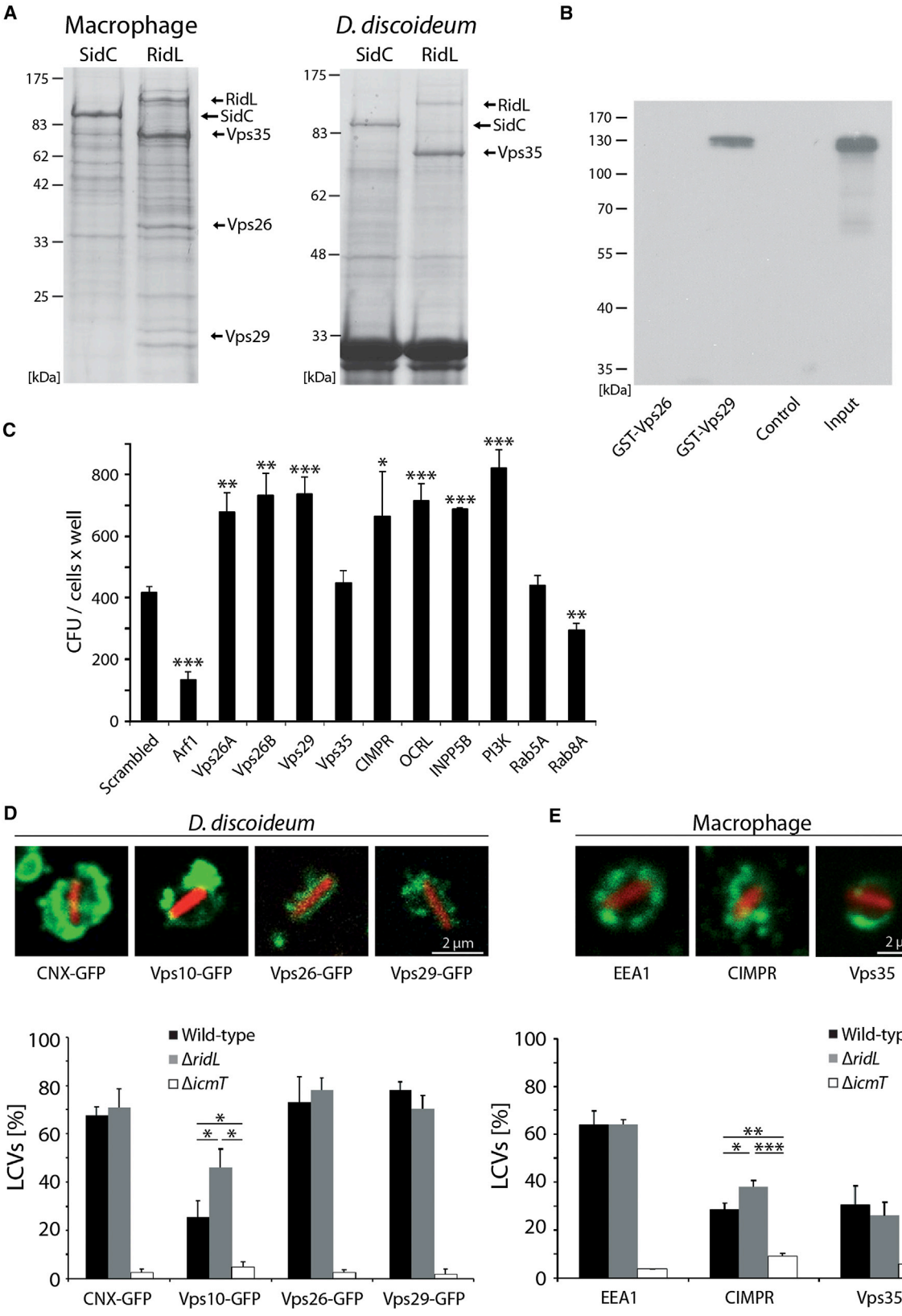

(legend on next page)

that RidL does not play a major role for the interaction of LCVs with vesicles trafficking along the secretory or endosomal pathway. In contrast, in comparison to LCVs containing WT *L. pneumophila*, significantly more Δ*ridL* LCVs accumulated the lysosomal marker LAMP-1 (Figure S3). Given that replication-permissive LCVs are LAMP-1-negative, this finding corresponds to the observation that in absence of *ridL* intracellular replication is reduced (Figure 1).

Finally, immunoaffinity-purified LCVs from *D. discoideum* infected with either WT or Δ*ridL L. pneumophila* were isolated in the same quantity (approximately 40% intact LCVs) and showed the same morphology and stability (Figure S3). This result suggests that RidL does not affect the overall integrity and stability of the LCV membrane. In summary, many known LCV markers accumulated to the same extent on LCVs harboring WT or Δ*ridL L. pneumophila*; yet, the retrograde cargo receptors Vps10/sortilin and CIMPR, as well as LAMP1, preferentially accumulated on Δ*ridL* LCVs. These findings support the notion that RidL promotes the formation of a nonlysosomal replicative pathogen vacuole by interfering with retrograde trafficking.

Sorting Nexins Accumulate on LCVs Harboring *L. pneumophila* Δ*ridL*

The retromer cargo recognition subcomplex interacts with membrane-associated SNXs to promote retrograde trafficking. Whereas the cargo recognition subunits were readily detected on LCV membranes (Figure 3), SNXs were barely detectable (SNX1 and SNX2) by fluorescence microscopy or not observed (SNX3) on LCVs in homogenates of RAW 264.7 macrophages (Figure 4A) or A549 lung epithelial cells ectopically producing GFP-SNX1 (Figure 4B). Similarly, SNX1 was hardly detectable by western blot in samples of intact purified LCVs from macrophages (Figure 4C). SNX5, on the other hand, was detected on 50% of the LCVs in macrophages (Figure 4A). Furthermore, western blot analysis indicated that RidL (but not SidC) coupled to beads retained the retromer cargo recognition subunit Vps35, but not SNX1, whereas, in macrophage lysates, Vps35 was barely detectable, and SNX1 was abundantly present (Figure 4D).

Interestingly, in the absence of *ridL*, approximately twice as many LCVs stained positive for SNX1 and SNX2 by fluorescence microscopy, whereas SNX3 was still not detectable, and the portion of SNX5-positive LCVs did not change (Figures 4A and 4B). Thus, we observed SNX1 on more than 50% of LCVs harboring *L. pneumophila* Δ*ridL* in homogenates of macrophages or A549 cells ectopically producing GFP-SNX1. Moreover, western blot analysis revealed a statistically significant 2-fold increase of SNX1 accumulation on purified LCVs harboring the Δ*ridL* mutant strain in comparison to WT *L. pneumophila* (Figure 4C). In summary, these results indicate that RidL promotes the removal of SNXs from the LCV membrane.

RidL Binds to PtdIns(3)*P* and Competes with SNXs for Membrane Binding

SNX1 and SNX2 localize to membranes by binding to PtdIns(3)*P*, and several *L. pneumophila* Icm/Dot substrates also bind to host PI lipids (Hilbi et al., 2011b). In a protein-lipid overlay assay, purified GST-RidL specifically bound to PtdIns(3)*P*, whereas GST-SidC selectively interacted with PtdIns(4)*P*, as was previously observed (Figure 4E).

To assess whether the PtdIns(3)*P*-binding effector RidL competes with SNX1 for membrane localization, we ectopically produced GFP-RidL in HeLa cells and quantified the colocalization of SNX1 with the endosomal marker transferrin receptor (TfR). The PtdIns(3)*P*-binding domain of the eukaryotic protein Hrs (GFP-2xFYVE) was used in parallel. Compared to cells producing GFP, significantly less SNX1 colocalized with TfR in cells ectopically producing GFP fusions with either PtdIns(3)*P*-binding protein (Figure 4F). Thus, two otherwise unrelated PtdIns(3)*P*-binding proteins compete with SNX1 for membrane localization, suggesting that PI binding is a major determinant of membrane localization of these proteins and providing a possible clue as to how RidL reduces the amount of SNXs on LCVs.

Ectopically Produced RidL Localizes to LCVs in *D. discoideum* and Mammalian Cells

To analyze the localization of heterologously expressed *ridL* in *L. pneumophila*-infected cells, we produced the protein in *D. discoideum* or HeLa cells and assessed its localization to LCVs. Stable heterologous production of RidL-GFP by *D. discoideum* was apparently not toxic for the amoeba (data not shown). Upon infection of *D. discoideum*-producing RidL-GFP with WT *L. pneumophila*, approximately 80% of the LCVs were uniformly decorated with RidL (Figure 5A).

HeLa cells transiently transformed for 24 hr with a plasmid encoding GFP-RidL produced a fusion protein of the expected molecular weight (~150 kDa, data not shown). Upon infection of the GFP-RidL-producing cells with WT *L. pneumophila*, approximately 60% of the LCVs were decorated with RidL

Figure 3. The Retromer Is Bound by RidL, Restricts Growth, and Localizes to LCVs

(A) RidL binds the retromer cargo recognition subcomplex. Affigel-10 beads coupled to recombinant RidL or SidC were incubated with lysates from RAW 264.7 macrophages or *D. discoideum*. Proteins eluting from washed beads were separated and identified by LC-ESI tandem mass spectrometry as retromer cargo recognition subcomplex subunits (Vps35, Vps29, and Vps26).

(B) RidL specifically binds Vps29. Purified GST-Vps26, but not GST-Vps29, retained RidL from *L. pneumophila* lysates as revealed by western blot with an antibody against RidL. Control, glutathione beads incubated with lysate; Input, lysate.

(C) Retromer inhibition promotes intracellular replication of *L. pneumophila*. HeLa cells were depleted for components of retrograde trafficking by RNAi (3 days), infected with *L. pneumophila* (MOI 20, 2 days), lysed, and intracellular replication of the bacteria was quantified by cfu. Data are representative of two to four of the four oligonucleotides used (complete set of data, see Figure S3).

(D and E) Role of RidL for localization of retromer subunits and cargo receptors on LCVs. *D. discoideum* producing GFP fusion proteins (D) or RAW 264.7 macrophages (E) were infected (MOI 25, 1 hr) with *L. pneumophila* WT, Δ*ridL*, or Δ*icmT* harboring pSW001. The presence on LCVs of retromer subunits (Vps29, Vps26, and Vps35), retrograde trafficking cargos (CIMPR, Vps10/sortilin), endosomal EEA1, or ER-derived calnexin was assessed by fluorescence microscopy in homogenates of infected cells.

Data in (C)–(E) represent means and SDs of three independent experiments (*$p < 0.05$; **$p < 0.01$; ***$p < 0.001$). Scale bars represent 2 μm. See also Figure S3.

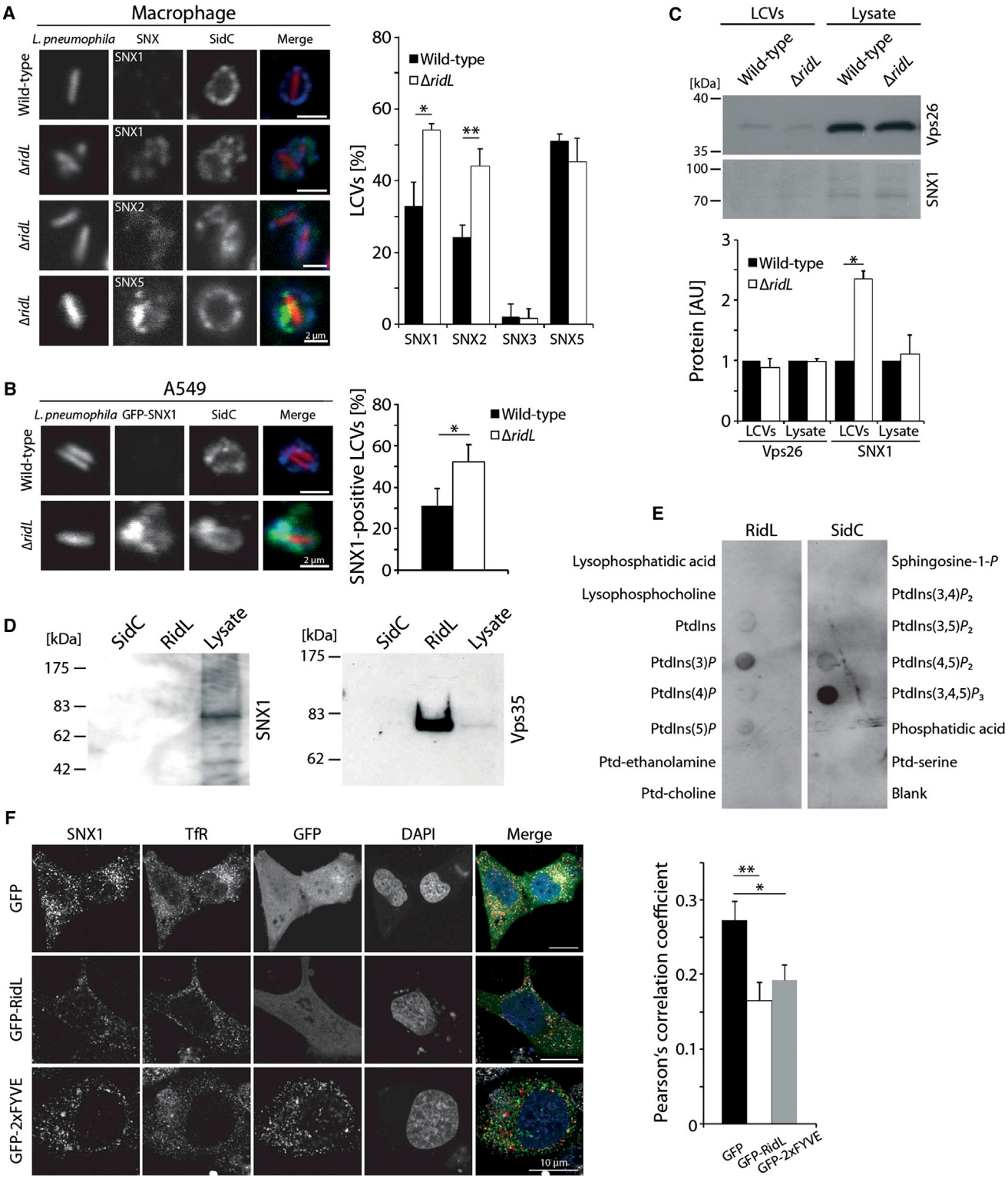

Figure 4. Sorting Nexins Accumulate on LCVs Harboring *L. pneumophila* Δ*ridL*

(A and B) SNX1 and SNX2 accumulate on LCVs in absence of *ridL*. RAW 264.7 macrophages (A) or A549 lung epithelial cells producing GFP-SNX1 (B) were infected (MOI 20 or 100, respectively) with *L. pneumophila* WT or Δ*ridL* containing pSW001 (DsRed) for 1 hr, homogenized, and SNX1, SNX2, SNX3, SNX5, or SidC were visualized by fluorescence microscopy.

(C) RidL decreases the binding of SNX1 to LCVs. RAW 264.7 macrophages were infected (MOI 50, 1 hr) with *L. pneumophila* WT or Δ*ridL* containing pSW001 (DsRed), and Vps26 or SNX1 were visualized and quantified by western blot in samples of purified LCVs or lysates (arbitrary units, AU).

(legend continued on next page)

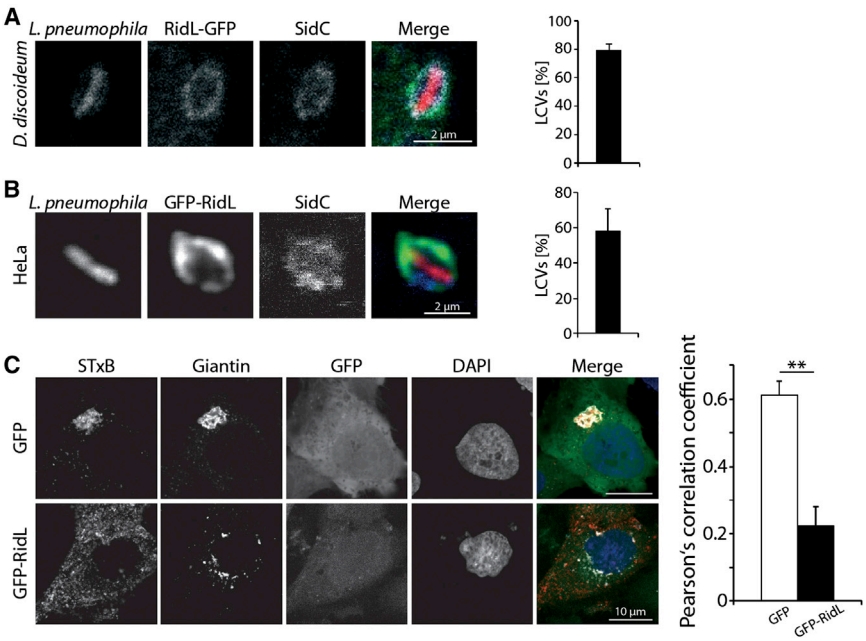

Figure 5. Localization and Retrograde Trafficking Inhibition of Ectopically Produced RidL

(A) *D. discoideum*-harboring pCR96 (RidL-GFP) was infected (MOI 25, 1 hr) with WT *L. pneumophila*/pSW001 (DsRed), and the presence of RidL on LCVs in intact cells was determined by fluorescence microscopy. Data are representative of three independent experiments (>50 LCVs each). The scale bar represents 2 μm.

(B) HeLa cells transiently transformed for 24 hr with plasmid pCR94 (GFP-RidL) were infected (MOI 100, 1hr) with WT *L. pneumophila*/pCR80 (DsRed and SidC), and GFP-RidL-positive LCVs were quantified in homogenates. Data represent means and SDs of three independent experiments (>50 LCVs each). The sale bar represents 2 μm.

(C) Inhibition of STxB trafficking in HeLa cells producing GFP-RidL. HeLa cells were transiently transformed for 24 hr with plasmid pCR94 (GFP-RidL) or pEGFP-C1 (GFP), and the trafficking of STxB-Cy3 was analyzed by colocalization with the Golgi marker giantin after 30 min. The Pearson's correlation coefficient was calculated in three independent experiments with >10 cells each (**p < 0.01). The scale bar represents 10 μm.

(Figure 5B). Altogether, these results indicate that ectopically produced fusion proteins of RidL and GFP localize to LCVs in infected amoeba or epithelial cells. Furthermore, localization of RidL to the LCV membrane does not require its translocation through a bacterial T4SS.

Ectopically Produced RidL Inhibits Retrograde Trafficking of Shiga Toxin

To investigate the effects of ectopically produced RidL on retrograde trafficking, we used HeLa cells, a well-established model for analyzing retrograde trafficking of shiga toxin that binds to a glycosphingolipid receptor termed globotriaosylceramide (Gb3/CD77). Transiently transformed cells produced GFP-RidL, which appeared to diffusely localize in the cytoplasm. The production of GFP-RidL was neither cytotoxic nor did it affect cell adherence, spreading, or morphology during the time course of the experiment (data not shown). The cells producing GFP-RidL were treated with fluorescently labeled receptor-binding subunit B of shiga toxin (STxB), and retrograde trafficking was assessed 30 min after treatment with the toxin (Figure 5C). In cells producing GFP-RidL, the fluorescently labeled STxB colocalized to a significantly lower extent with the Golgi marker giantin in comparison to cells producing GFP. This result establishes the *L. pneumophila* effector protein RidL as an inhibitor of the eukaryotic retrograde vesicle trafficking pathway.

RidL Inhibits Retrograde Trafficking in *L. pneumophila*-Infected Macrophages

To test whether RidL interferes with the retrograde pathway in *L. pneumophila*-infected macrophages, we followed the uptake and trafficking of fluorescently labeled subunit B of cholera toxin (CTxB), which interacts with the glycosphingolipid receptor GM1 present on RAW 264.7 macrophages and reaches the target cell cytoplasm via the retrograde route. The macrophages were infected with *L. pneumophila* WT, Δ*icmT*, Δ*ridL*, or a complemented *ridL* mutant strain for 1 hr and, subsequently, were incubated with red fluorescent CTxB-AlexaFluor555 for 10, 30, or 60 min. For the time of the experiment, the morphology and adherence of the infected macrophages was similar for all bacterial strains (data not shown).

In comparison to uninfected cells, retrograde trafficking of CTxB was compromised in macrophages previously infected with WT *L. pneumophila* (Figure 6A; see also Figure S4). However, in macrophages infected with *L. pneumophila* lacking *ridL*, the retrograde transport of CTxB was no longer blocked, indicating that RidL is required for inhibiting the retrograde pathway. Whereas 85% of the macrophages infected for 10 or

(A–C) Data in represent means and SDs of three independent experiments, scoring > 40 LCVs each (A and B) or quantifying protein amounts by densitometry (C) (*p < 0.05; **p < 0.01). Scale bars represent 2 μm.

(D) RidL binds the retromer cargo recognition subcomplex, but not SNX1. RidL or SidC bound to Affigel-10 beads were incubated with lysates from RAW 264.7 macrophages and washed. The eluate was subjected to western blotting with antibodies against SNX1 or Vps35 and horseradish peroxidase-coupled secondary. Control, lysate.

(E) Protein-lipid overlay using different lipids (160 pmol) spotted in two columns on nitrocellulose membranes and affinity-purified GST-RidL or GST-SidC. Binding to PtdIns(3)*P* or PtdIns(4)*P*, respectively, was visualized with an antibody against GST. PtdIns, phosphatidylinositol.

(F) Competition of RidL or 2xFYVE with SNX1 for binding to PtdIns(3)*P*. In HeLa cells ectopically producing GFP-RidL, GFP-2xFYVE, or GFP. Colocalization of SNX1 with the endosomal marker transferrin receptor (TfR) was scored. The Pearson's correlation coefficient was calculated in three independent experiments with 10 cells each (*p < 0.05; **p < 0.01). The scale bar represents 10 μm.

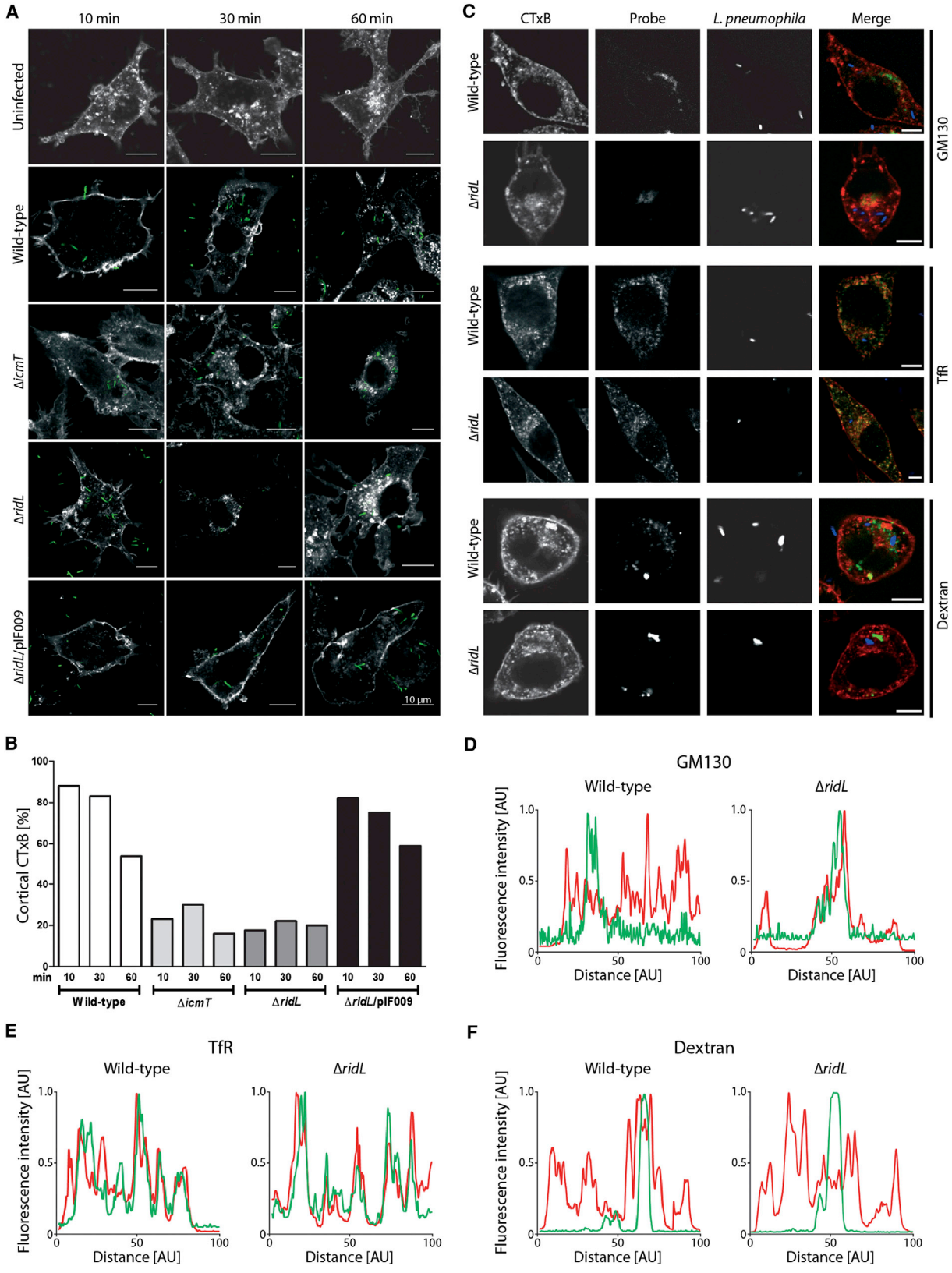

(legend on next page)

30 min with WT *L. pneumophila* showed a peripheral localization of CTxB, only 20% of the macrophages infected with the Δ*ridL* mutant strain showed impaired retrograde trafficking of CTxB (Figure 6B). This phenotype of the Δ*ridL* strain was restored to the WT level (i.e., inhibition of retrograde transport) upon complementation of the mutant by supplying *ridL* on a plasmid. *L. pneumophila* lacking a functional Icm/Dot T4SS did not inhibit retrograde trafficking, which was in agreement with the finding that RidL is an Icm/Dot substrate. Altogether, these findings establish the Icm/Dot-translocated effector RidL as a bacterial inhibitor of the retrograde vesicle trafficking pathway in *L. pneumophila*-infected eukaryotic cells.

Furthermore, we analyzed the subcellular localization of CTxB upon the inhibition of retrograde trafficking by *L. pneumophila*. To this end, RAW 264.7 macrophages were infected with WT or Δ*ridL L. pneumophila* and incubated with CTxB in presence of the lysosome marker dextran-AlexaFluor647 or immunostained for the Golgi apparatus (GM130) or early and recycling endosomes (TfR), respectively. In macrophages infected with WT *L. pneumophila*, colocalization of CTxB was detected for TfR, but barely for GM130 or dextran (Figure 6C). Colocalization was quantified by analyzing the fluorescence intensity along a section of the infected and toxin-treated macrophages (Figures 6D–6F; see also Figure S4). In contrast, in macrophages infected with Δ*ridL*, CTxB colocalized with early and recycling endosomal compartments as well as the Golgi apparatus but barely colocalized with lysosomes (Figures 6D–6F and S4). These observations are consistent with the notion that *L. pneumophila* blocks retrograde trafficking in a RidL-dependent manner at endosome exit sites; i.e., at a postendosome or pre-Golgi stage, which is the step executed by the retromer complex. The findings are also in agreement with the idea that RidL inhibits the activity of the retromer complex. We did not detect colocalization of CTxB with LCVs harboring either WT or Δ*ridL L. pneumophila*, indicating that, on its retrograde trafficking route, the toxin bypassed the pathogen vacuole (data not shown).

Collectively, the findings presented here show that the inhibition of retrograde trafficking in amoeba and mammalian cells by *L. pneumophila* promotes intracellular bacterial replication and, thus, shed light on the conserved virulence strategy of the pathogen. Moreover, we identified and characterized the Icm/Dot-translocated effector protein RidL as an interactor of the eukaryotic retromer cargo recognition subcomplex. By binding to Vps29 and the PI lipid PtdIns(3)*P*, RidL may interfere with the assembly of a functional retromer complex and prevent productive interactions of the retromer cargo recognition subcomplex with SNXs and/or with other retromer interactors (Figure 7). These findings pave the way for further analysis of the cellular functions, composition, assembly, dynamics, and regulation of the retromer complex and retrograde vesicle trafficking.

DISCUSSION

The formation of a replication-permissive LCV is a complex and robust process that requires the bacterial Icm/Dot T4SS and involves close to 300 distinct effector proteins that are translocated into the host cell. In this study, we characterized the *L. pneumophila* effector protein RidL as a bacterial interactor of the eukaryotic retromer complex. RidL blocks retrograde trafficking and, thus, promotes intracellular bacterial replication.

In pulldown experiments, RidL interacted with the cargo recognition subcomplex Vps35-Vps29-Vps26 of the eukaryotic retromer and the effector protein bound the 20 kDa subunit Vps29, but not Vps26, in vitro. Whereas RidL specifically binds Vps29, a herpesvirus saimiri protein termed Tip was found to interact with Vps35 (Kingston et al., 2011). This interaction caused a redistribution of Vps35 from early endosomes to lysosomes and strongly inhibited retromer activity. However, retromer inhibition did not directly affect the rate of intracellular viral replication.

LCV markers implicated in the retrograde vesicle trafficking pathway include the cargo receptors Vps10/sortilin and CIMPR as well as the components of the retromer cargo recognition subcomplex. The Vps29 retromer subunit was previously identified on LCVs isolated from *L. pneumophila*-infected *D. discoideum* with a proteomics approach (Shevchuk et al., 2009). Upon depletion of CIMPR, Vps26A/B or Vps29 intracellular *L. pneumophila* grew more efficiently in comparison to the control with scrambled siRNA.

The PI phosphatase OCRL represents another LCV marker involved in retrograde trafficking (Weber et al., 2009a). *L. pneumophila* replicates more efficiently upon depletion of several PI-metabolizing enzymes implicated in retrograde vesicle trafficking, namely the PI 5-phosphatases OCRL and INPP5B, as well as PI3K. These findings correspond to previous studies showing that, in *D. discoideum*, the deletion of the OCRL homolog Dd5P4 or PI3Ks enhances intracellular growth of *L. pneumophila* (Weber et al., 2009a; Weber et al., 2006).

The small GTPase Rab7 promotes late steps of the endocytic pathway and was identified on *D. discoideum* LCVs by proteomics and as a GFP fusion protein (Urwyler et al., 2009). Rab7 also represents an important regulator of retrograde trafficking in mammalian cells (Rojas et al., 2008) as well as in the protozoon *Entamoeba histolytica* (Nakada-Tsukui et al., 2005). The active

Figure 6. *L. pneumophila* RidL Inhibits Retrograde Trafficking at Endosome Exit Sites

(A) RidL inhibits retrograde trafficking of CTxB in macrophages. Fluorescence images of uninfected RAW 264.7 macrophages or infected (MOI 50, 1 hr) with *L. pneumophila* WT, Δ*icmT*, or Δ*ridL* harboring pNT28 (GFP) or complemented Δ*ridL*/pIF009 (GFP and RidL) followed by incubation with CTxB-AlexaFluor555 (gray scale) for 10, 30, or 60 min. Control, uninfected macrophages. Scale bars represent 10 μm.

(B) Quantification of peripheral CTxB in *L. pneumophila*-infected macrophages. The percentage of 100 macrophages depicted in (A) that show a peripheral localization of CTxB-AlexaFluor555 (retrograde trafficking defect) is indicated. Data are representative of three independent experiments.

(C–F) CTxB localizes to endosomes in *Legionella*-infected cells. RAW 264.7 macrophages were infected (MOI 50, 1 hr) with *L. pneumophila* WT or Δ*ridL* harboring pNT28 (GFP, shown in blue) and were incubated with CTxB-AlexaFluor555 (red) for 45 min in presence of dextran-AlexaFluor647 or analyzed by immunostaining (Cy5, shown in green) with antibodies against GM130 or TfR.

(D–F) Overlays of the standardized relative fluorescence intensity (arbitrary units, AU) along a section of CTxB (red) with GM130, TfR, or dextran, respectively (green). Representative cells from three independent experiments are shown. The scale bars represent 5 μm.

See also Figure S4.

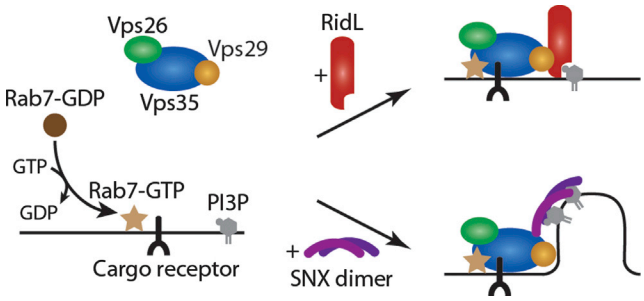

Figure 7. Model of the Inhibitory Mechanism of RidL
LCVs harboring WT or Δ*ridL L. pneumophila* are decorated with Rab7, the Vps26-Vps29-Vps35 retromer cargo recognition subcomplex, and sorting nexin dimers. RidL inhibits retrograde transport and binds to Vps29 as well as to PtdIns(3)*P* and, thus, directly or indirectly interferes with the assembly of a functional retromer complex, competes with sorting nexin dimers for membrane localization, and/or inhibits the interaction with sorting nexins or other retromer effectors.

GTP-bound form of Rab7 interacts with the retromer cargo recognition subcomplex and, thus, along with SNXs, is a coreceptor for the retromer. Depletion of Rab7 or a dominant-negative form of the GTPase caused the retromer cargo recognition subcomplex, but not the SNX dimer, to dissociate from endosomes (Rojas et al., 2008).

RidL is dispensable for the recruitment to LCVs of the retromer and other factors implicated in retrograde trafficking, such as Dd5P4/OCRL or Rab7. Consequently, RidL does not appear to be an analog of the mammalian SNX dimer, which promotes the membrane recruitment of the retromer cargo recognition subcomplex (Rojas et al., 2007). Yet, compared to LCVs harboring WT *L. pneumophila*, significantly more LCVs harboring Δ*ridL* mutants accumulated the retrograde trafficking receptors Vps10/sortilin and CIMPR, suggesting that RidL interferes with retrograde trafficking. Accordingly, ectopically produced RidL indeed inhibited retrograde trafficking of STxB in HeLa cells, and WT, but not Δ*ridL*, mutant *L. pneumophila* prevented retrograde trafficking of CTxB in macrophages. These results are in agreement with the notion that RidL is a retromer inhibitor that promotes the intracellular replication of *L. pneumophila*.

In presence of RidL, CTxB preferentially colocalized with early and recycling endosomal compartments rather than with the Golgi apparatus. Thus, *L. pneumophila* blocks the retrograde pathway in a RidL-dependent manner at a postendosome or pre-Golgi stage, which is the very step executed by the retromer complex. Again, this finding supports the notion that RidL inhibits retromer activity. Notably, CTxB did not colocalize with LCVs harboring either WT or Δ*ridL L. pneumophila*, suggesting that the toxin bypassed the pathogen vacuole and RidL interacts with the retromer in *cis* (directly on the LCV) as well as in *trans* (on separate donor compartments of the retrograde pathway).

The sorting nexins SNX1, SNX2, and SNX5, but not SNX3, localize to LCVs. SNX1 and SNX2 accumulated on a significantly larger number of LCVs harboring Δ*ridL*, whereas, in the absence of *ridL*, the number of SNX5-positive LCVs did not change, and SNX3 was still not detected. Treatment with siRNA oligonucleotides targeting SNX1, −2, −3, or −5 alone or two of the SNXs in combination did not affect the intracellular growth of *L. pneumophila*. Perhaps other SNXs among the 33 known mammalian family members (Cullen, 2008) are relevant for intracellular replication of *L. pneumophila*. Alternatively, the retromer effector involved in the growth of *L. pneumophila* is not a SNX but another host factor. In this context, it is interesting to note that pathogen vacuoles containing *Salmonella enterica* Typhimurium acquire both SNX1 and SNX3 at early stages of infection, and these SNXs appear to play a role for intracellular replication of the pathogen (Braun et al., 2010; Bujny et al., 2008).

SNX1 and SNX2 localize to membranes by binding through PX domains to PtdIns(3)*P* (Carlton et al., 2004; Cullen and Korswagen, 2012). The Icm/Dot-translocated effectors RidL and SetA (Jank et al., 2012) also bind to PtdIns(3)*P*. Therefore, these (and perhaps other) *L. pneumophila* effectors might compete with SNXs on LCVs by interacting with PI lipids. In support of this notion, ectopically produced GFP-RidL, as well as GFP-2xFYVE, competed with SNX1 on endosomal membranes. Alternatively or additionally, by binding to the retromer subunit Vps29, RidL might prevent a productive interaction between the retromer cargo recognition subcomplex and SNXs or other retromer interactors, such as the Rab GTPase-activating protein (GAP) TBC1D5 (Seaman et al., 2009). Such an inhibitory mechanism is in agreement with the notion that SNXs bind to membranes independently of the retromer cargo recognition subcomplex (Rojas et al., 2007). Our current working model of the mode of action of RidL encompasses the possible competition of RidL with SNXs for LCV localization by binding to PtdIns(3)*P* and/or by binding to Vps29, the inhibition of a productive interaction between the retromer cargo recognition subcomplex and SNXs or other retromer interactors.

In summary, we have shown that *L. pneumophila* inhibits retrograde trafficking and that the inhibition of retrograde trafficking promotes intracellular replication. Moreover, we characterized the Icm/Dot-translocated effector protein RidL as a bacterial interactor of the eukaryotic retromer complex. These findings pave the way for further analysis of the cellular functions, composition, assembly, dynamics, and regulation of the retromer complex and the retrograde vesicle trafficking pathway.

EXPERIMENTAL PROCEDURES

Cells, Bacteria, and Plasmids

Host cells, *Legionella pneumophila* strains, plasmids, and oligonucleotides are listed in Tables S1 and S2. Chromosomal deletion of *ridL* was performed as previously described (Tiaden et al., 2007) and is detailed in the Supplemental Experimental Procedures along with the construction of plasmids.

Protein Purification and Antibody Production

GST fusion proteins were produced and cleaved with PreScission Protease according to the manufacturer's recommendations (Amersham Pharmacia). His-tagged RidL encoded by plasmid pCR5 was purified by nickel affinity chromatography and used to raise a polyclonal antibody in rabbits as previously described (Weber et al., 2006).

Pulldown Experiments

Pulldown experiments with purified RidL or SidC covalently linked to Affigel-10 beads were performed as previously described (Ragaz et al., 2008; Weber et al., 2006). In brief, RidL- or SidC-coupled beads were incubated with lysate of RAW 264.7 macrophages or *D. discoideum*. Eluted host proteins were separated by SDS-PAGE and identified by liquid chromatography-electrospray ionization tandem mass spectrometry (LC-ESI-MS/MS). Pulldown experiments using GST-Vps26 or GST-Vps29 were performed with lysates of

L. pneumophila overproducing RidL (pIF007), and binding was visualized by western blot with a polyclonal antibody against RidL.

Protein-Lipid Overlay

The binding of GST-RidL or GST-SidC to PIs and other lipids was tested in protein-lipid overlay assays using commercially available PIP strips (Echelon Biosciences) as previously described (Weber et al., 2006).

Intracellular Trafficking and (Immuno-)Fluorescence Microscopy

Fluorescence microscopy with RAW 264.7 macrophages or *D. discoideum* producing GFP fusion proteins as well as quantitation of LCV markers were performed as previously described (Ragaz et al., 2008; Weber et al., 2009a; Weber et al., 2006). In order to obtain mammalian cells that produce GFP-SNX1, A549 lung epithelial cells were transiently transfected by lipofection with plasmid pEGFP-C1-SNX1.

Retrograde trafficking was analyzed in RAW 264.7 macrophages infected (MOI 50, 1 hr, 37°C) with GFP-producing *L. pneumophila* strains, washed with PBS, and treated with fluorescently labeled CTxB (CTxB-AlexaFluor555, Molecular Probes) at 0.5 μg/ml (5 min on ice, 10–60 min at 37°C) prior to fixation (4% paraformaldehyde, 20 min, RT). Where indicated, CTxB was incubated along with dextran-AlexaFluor647 (1:125, Molecular Probes), or, after fixation, the infected macrophages were immunostained with antibodies against GM130 (1:200, BD Biosciences) or TfR (1:100, Abcam) and secondary anti-mouse or anti-rabbit Cy5-coupled antibodies.

Alternatively, HeLa cells were transiently transformed for 24 hr with plasmid pEGFP-N1-*ridL* (pCR093), pEGFP-C1-*ridL* (pCR094), or pEGFP-C1 encoding RidL-GFP, GFP-RidL, or GFP, respectively. Retrograde trafficking and intracellular distribution of fluorescently labeled STxB (STxB-Cy3) (Mallard et al., 1998) was monitored. Toxin localization was scored by either calculating the Pearson's correlation coefficient for colocalization with marker proteins or by determining the toxin distribution between the cell cortex and perinuclear compartments.

Intracellular Growth Assays

Single-infection-cycle intracellular growth of GFP-producing *L. pneumophila* in RAW 264.7 macrophages or *A. castellanii* amoeba and coinfection competition assays in *A. castellanii* was analyzed as previously described (Kessler et al., 2013). Fibroblasts from Lowe syndrome patients or healthy individuals were seeded in 96-well plates (10^4 cells), left to adhere overnight, and infected with *L. pneumophila* (MOI 20) for 3 hr. The infected cells were washed three times with Dulbecco's modified Eagle's medium, and, after 3 or 6 days, the cells were lysed with 0.8% saponin, and intracellular bacteria were quantified as cfu.

RNAi

RNAi experiments were performed with epithelial cells cultured in 96-well plates and treated with a final concentration of 20 nM (HeLa, 3 days) or 10 nM (A549, 2 days) of the indicated siRNA oligonucleotides (Table S3).

SUPPLEMENTAL INFORMATION

Supplemental Information contains Supplemental Experimental Procedures, four figures, and three tables and can be found with this article online at http://dx.doi.org/10.1016/j.chom.2013.06.001.

ACKNOWLEDGMENTS

We would like to thank G. Pfaffinger for superb technical assistance. S. Heiny helped with cloning and the adenylate cyclase assay. S. Höning (University of Köln), P. Cullen (University of Bristol), and H. Stenmark (Oslo University Hospital) kindly provided an antibody against CIMPR, plasmid pEGFP-C1-SNX1, or the GFP-2xFYVE construct, respectively. Research was funded by the Max von Pettenkofer Institute, LMU Munich, the German Research Foundation (HI 1511/1-1, SPP1580, SFB914, and GRK1459), the BMBF (Medical Infection Genomics initiative, 0315834C), and the Swiss National Science Foundation (31003A-125369; CRSI33_130016).

Received: July 6, 2012
Revised: March 28, 2013
Accepted: May 16, 2013
Published: July 17, 2013

REFERENCES

Arighi, C.N., Hartnell, L.M., Aguilar, R.C., Haft, C.R., and Bonifacino, J.S. (2004). Role of the mammalian retromer in sorting of the cation-independent mannose 6-phosphate receptor. J. Cell Biol. *165*, 123–133.

Bonifacino, J.S., and Hurley, J.H. (2008). Retromer. Curr. Opin. Cell Biol. *20*, 427–436.

Bonifacino, J.S., and Rojas, R. (2006). Retrograde transport from endosomes to the trans-Golgi network. Nat. Rev. Mol. Cell Biol. *7*, 568–579.

Braun, V., Wong, A., Landekic, M., Hong, W.J., Grinstein, S., and Brumell, J.H. (2010). Sorting nexin 3 (SNX3) is a component of a tubular endosomal network induced by *Salmonella* and involved in maturation of the *Salmonella*-containing vacuole. Cell. Microbiol. *12*, 1352–1367.

Brombacher, E., Urwyler, S., Ragaz, C., Weber, S.S., Kami, K., Overduin, M., and Hilbi, H. (2009). Rab1 guanine nucleotide exchange factor SidM is a major phosphatidylinositol 4-phosphate-binding effector protein of *Legionella pneumophila*. J. Biol. Chem. *284*, 4846–4856.

Bujny, M.V., Ewels, P.A., Humphrey, S., Attar, N., Jepson, M.A., and Cullen, P.J. (2008). Sorting nexin-1 defines an early phase of *Salmonella*-containing vacuole-remodeling during *Salmonella* infection. J. Cell Sci. *121*, 2027–2036.

Carlton, J., Bujny, M., Peter, B.J., Oorschot, V.M., Rutherford, A., Mellor, H., Klumperman, J., McMahon, H.T., and Cullen, P.J. (2004). Sorting nexin-1 mediates tubular endosome-to-TGN transport through coincidence sensing of high- curvature membranes and 3-phosphoinositides. Curr. Biol. *14*, 1791–1800.

Chien, M., Morozova, I., Shi, S., Sheng, H., Chen, J., Gomez, S.M., Asamani, G., Hill, K., Nuara, J., Feder, M., et al. (2004). The genomic sequence of the accidental pathogen *Legionella pneumophila*. Science *305*, 1966–1968.

Clemens, D.L., Lee, B.Y., and Horwitz, M.A. (2000). *Mycobacterium tuberculosis* and *Legionella pneumophila* phagosomes exhibit arrested maturation despite acquisition of Rab7. Infect. Immun. *68*, 5154–5166.

Cullen, P.J. (2008). Endosomal sorting and signalling: an emerging role for sorting nexins. Nat. Rev. Mol. Cell Biol. *9*, 574–582.

Cullen, P.J., and Korswagen, H.C. (2012). Sorting nexins provide diversity for retromer-dependent trafficking events. Nat. Cell Biol. *14*, 29–37.

Hilbi, H., and Haas, A. (2012). Secretive bacterial pathogens and the secretory pathway. Traffic *13*, 1187–1197.

Hilbi, H., Hoffmann, C., and Harrison, C.F. (2011a). *Legionella* spp. outdoors: colonization, communication and persistence. Environ Microbiol Rep *3*, 286–296.

Hilbi, H., Weber, S., and Finsel, I. (2011b). Anchors for effectors: subversion of phosphoinositide lipids by *legionella*. Front Microbiol *2*, 91.

Huang, L., Boyd, D., Amyot, W.M., Hempstead, A.D., Luo, Z.Q., O'Connor, T.J., Chen, C., Machner, M., Montminy, T., and Isberg, R.R. (2011). The E Block motif is associated with *Legionella pneumophila* translocated substrates. Cell. Microbiol. *13*, 227–245.

Hubber, A., and Roy, C.R. (2010). Modulation of host cell function by *Legionella pneumophila* type IV effectors. Annu. Rev. Cell Dev. Biol. *26*, 261–283.

Isberg, R.R., O'Connor, T.J., and Heidtman, M. (2009). The *Legionella pneumophila* replication vacuole: making a cosy niche inside host cells. Nat. Rev. Microbiol. *7*, 13–24.

Jank, T., Böhmer, K.E., Tzivelekidis, T., Schwan, C., Belyi, Y., and Aktories, K. (2012). Domain organization of *Legionella* effector SetA. Cell. Microbiol. *14*, 852–868.

Johannes, L., and Popoff, V. (2008). Tracing the retrograde route in protein trafficking. Cell *135*, 1175–1187.

Kagan, J.C., Stein, M.P., Pypaert, M., and Roy, C.R. (2004). *Legionella* subvert the functions of Rab1 and Sec22b to create a replicative organelle. J. Exp. Med. *199*, 1201–1211.

Kessler, A., Schell, U., Sahr, T., Tiaden, A., Harrison, C., Buchrieser, C., and Hilbi, H. (2013). The *Legionella pneumophila* orphan sensor kinase LqsT regulates competence and pathogen-host interactions as a component of the LAI-1 circuit. Environ. Microbiol. *15*, 646–662.

Kingston, D., Chang, H., Ensser, A., Lee, H.R., Lee, J., Lee, S.H., Jung, J.U., and Cho, N.H. (2011). Inhibition of retromer activity by herpesvirus saimiri tip leads to CD4 downregulation and efficient T cell transformation. J. Virol. *85*, 10627–10638.

Lowe, M. (2005). Structure and function of the Lowe syndrome protein OCRL1. Traffic *6*, 711–719.

Luo, Z.Q., and Isberg, R.R. (2004). Multiple substrates of the *Legionella pneumophila* Dot/Icm system identified by interbacterial protein transfer. Proc. Natl. Acad. Sci. USA *101*, 841–846.

Mallard, F., Antony, C., Tenza, D., Salamero, J., Goud, B., and Johannes, L. (1998). Direct pathway from early/recycling endosomes to the Golgi apparatus revealed through the study of shiga toxin B-fragment transport. J. Cell Biol. *143*, 973–990.

Nakada-Tsukui, K., Saito-Nakano, Y., Ali, V., and Nozaki, T. (2005). A retromer-like complex is a novel Rab7 effector that is involved in the transport of the virulence factor cysteine protease in the enteric protozoan parasite *Entamoeba histolytica*. Mol. Biol. Cell *16*, 5294–5303.

Newton, H.J., Ang, D.K., van Driel, I.R., and Hartland, E.L. (2010). Molecular pathogenesis of infections caused by *Legionella pneumophila*. Clin. Microbiol. Rev. *23*, 274–298.

Ragaz, C., Pietsch, H., Urwyler, S., Tiaden, A., Weber, S.S., and Hilbi, H. (2008). The *Legionella pneumophila* phosphatidylinositol-4 phosphate-binding type IV substrate SidC recruits endoplasmic reticulum vesicles to a replication-permissive vacuole. Cell. Microbiol. *10*, 2416–2433.

Rivero, F., Kuspa, A., Brokamp, R., Matzner, M., and Noegel, A.A. (1998). Interaptin, an actin-binding protein of the alpha-actinin superfamily in *Dictyostelium discoideum*, is developmentally and cAMP-regulated and associates with intracellular membrane compartments. J. Cell Biol. *142*, 735–750.

Rojas, R., Kametaka, S., Haft, C.R., and Bonifacino, J.S. (2007). Interchangeable but essential functions of SNX1 and SNX2 in the association of retromer with endosomes and the trafficking of mannose 6-phosphate receptors. Mol. Cell. Biol. *27*, 1112–1124.

Rojas, R., van Vlijmen, T., Mardones, G.A., Prabhu, Y., Rojas, A.L., Mohammed, S., Heck, A.J., Raposo, G., van der Sluijs, P., and Bonifacino, J.S. (2008). Regulation of retromer recruitment to endosomes by sequential action of Rab5 and Rab7. J. Cell Biol. *183*, 513–526.

Seaman, M.N. (2004). Cargo-selective endosomal sorting for retrieval to the Golgi requires retromer. J. Cell Biol. *165*, 111–122.

Seaman, M.N. (2005). Recycle your receptors with retromer. Trends Cell Biol. *15*, 68–75.

Seaman, M.N., Harbour, M.E., Tattersall, D., Read, E., and Bright, N. (2009). Membrane recruitment of the cargo-selective retromer subcomplex is catalysed by the small GTPase Rab7 and inhibited by the Rab-GAP TBC1D5. J. Cell Sci. *122*, 2371–2382.

Shevchuk, O., Batzilla, C., Hägele, S., Kusch, H., Engelmann, S., Hecker, M., Haas, A., Heuner, K., Glöckner, G., and Steinert, M. (2009). Proteomic analysis of *Legionella*-containing phagosomes isolated from *Dictyostelium*. Int. J. Med. Microbiol. *299*, 489–508.

Tiaden, A., Spirig, T., Weber, S.S., Brüggemann, H., Bosshard, R., Buchrieser, C., and Hilbi, H. (2007). The *Legionella pneumophila* response regulator LqsR promotes host cell interactions as an element of the virulence regulatory network controlled by RpoS and LetA. Cell. Microbiol. *9*, 2903–2920.

Urwyler, S., Nyfeler, Y., Ragaz, C., Lee, H., Mueller, L.N., Aebersold, R., and Hilbi, H. (2009). Proteome analysis of *Legionella* vacuoles purified by magnetic immunoseparation reveals secretory and endosomal GTPases. Traffic *10*, 76–87.

Weber, S.S., Ragaz, C., Reus, K., Nyfeler, Y., and Hilbi, H. (2006). *Legionella pneumophila* exploits PI(4)*P* to anchor secreted effector proteins to the replicative vacuole. PLoS Pathog. *2*, e46.

Weber, S.S., Ragaz, C., and Hilbi, H. (2009a). The inositol polyphosphate 5-phosphatase OCRL1 restricts intracellular growth of *Legionella*, localizes to the replicative vacuole and binds to the bacterial effector LpnE. Cell. Microbiol. *11*, 442–460.

Weber, S.S., Ragaz, C., and Hilbi, H. (2009b). Pathogen trafficking pathways and host phosphoinositide metabolism. Mol. Microbiol. *71*, 1341–1352.

Zhu, W., Banga, S., Tan, Y., Zheng, C., Stephenson, R., Gately, J., and Luo, Z.Q. (2011). Comprehensive identification of protein substrates of the Dot/Icm type IV transporter of *Legionella pneumophila*. PLoS ONE *6*, e17638.

Zusman, T., Aloni, G., Halperin, E., Kotzer, H., Degtyar, E., Feldman, M., and Segal, G. (2007). The response regulator PmrA is a major regulator of the icm/dot type IV secretion system in *Legionella pneumophila* and *Coxiella burnetii*. Mol. Microbiol. *63*, 1508–1523.